Hindawi
Mathematical Problems in Engineering
Volume 2022, Article ID 1265658, 11 pages
https://doi.org/10.1155/2022/1265658

Research Article

Two-Dimensional Transceiver Beamforming for Mainlobe Jamming Suppression with FDA-MIMO Radar

Pengfei Wan,[1,2] **Guisheng Liao**,[1] **Jingwei Xu**,[1] **and Guimei Zheng**[2]

[1]*National Laboratory of Radar Signal Processing, Xidian University, Xi'an, Shaanxi 710071, China*
[2]*Air Defence and Anti Missile College, Air Force Engineering University, Xi'an, Shaanxi 710051, China*

Correspondence should be addressed to Pengfei Wan; wanpengfei@stu.xidian.edu.cn

Received 7 March 2022; Revised 3 April 2022; Accepted 11 June 2022; Published 8 July 2022

Academic Editor: Ardashir Mohammadzadeh

With the rapid development of electronic warfare technology, the airborne electronic counter measures (ECM) system can generate mainlobe jamming using range gate pull-off (RGPO) strategy, which brings serious performance degradation of target tracking for the tracking and guidance radar. In this study, a two-dimensional transceiver beamforming approach is proposed to suppress the mainlobe jamming with frequency diverse array using multiple-input multiple-output (FDA-MIMO) radar. The mainlobe jamming signal differs from the real target echo in the joint transmit and receive domain due to the range dependence of FDA beampattern. The amplitude of RGPO signal is greater than the amplitude of real target echo. Thus, the transceiver beampattern can be designed to null out the jamming while maintaining the real target. The jamming suppression performance is studied in consideration of practical range constraint of RGPO. Simulation results are provided to verify the effectiveness of the proposed approach.

1. Introduction

Tracking and guidance radar plays an important role in national defense applications [1–4]. It provides sufficient antijamming ability against the jammers with the low side lobe antenna technique and large time-bandwidth products. However, with the development of electronic interference technique in the advanced weapons, tracking and guidance radar encounters extremely hostile environment in the mainlobe [5–7]. For example, the electronic counter measures (ECM) system has been developed to generate strong jamming in the mainlobe [8–10], which becomes a great challenge for the traditional phased array radar systems.

The mainlobe jamming is not easy to implement and also difficult to suppress. Especially, the multidimensional modulation deceptive jamming signal from the mainlobe seriously affects the performance of the radar system [11–14]. Deceptive jamming intercepts the radiation signal of radar by airborne electronic support measures (ESM) and modulates the range and speed in multiple dimensions, and then a deceptive jamming pattern similar to the real radar detection waveform is generated, that is, the false target is generated by the way of "intercept-modulation-forward," which can make the radar system mistakenly regard the false target as the real target. Therefore, deceptive jamming has serious consequences such as increased false alarm, missing of real target, and extremely heavy computational burden [15–17].

RGPO is an effective technique for deceptive jamming of radar range information. Because it has the advantages of low interference power and strong flexibility, it has become a hot research topic in recent years [18, 19]. Greco et al. [20] studied the working mechanism of RGPO and analyzed the influence of delay quantization based on digital radio frequency memory (DRFM) on jamming signals. Öztürk et al. [21] adopted the RGPO of bidirectional false target, which can effectively resist the pulse leading edge or trailing edge tracking technology adopted by radar. Xie et al. [22] proposed a range gate RGPO method based on bidirectional false targets, which is verified by evaluating radar measurements. In the study by Rui-xing and Jian-yun [23], a jamming power compensation technique was proposed to

improve the success rate of range gate RGPO, and the output peak value of pulse compression was used to evaluate the RGPO effect. Xue and Yang [24] optimized the realization mode of range gate RGPO and put forward a method to improve the effect of range gate RGPO by frequency shift technology.

In order to counter the RGPO, this study presents a method of countering the range gate RGPO based on frequency diverse array (FDA)-multiple-input multiple-output (MIMO) radar [25]. It is a new radar system that combines frequency diversity array and MIMO radar [26–29]. Because of the multiantenna transmission single frequency step system, it forms a three-dimensional range-angle-time-dependent pattern in the far field, and the research shows that the range-angle dependence of FDA's transmission pattern is different from that of traditional radar [30]. However, in order to make full use of this characteristic, it is necessary to effectively separate the transmitter signal, and MIMO radar technology is an effective means to obtain the freedom of transmission [31]. Zhang and Xie [32] extracted the phase difference of adjacent array elements by analyzing the influence of each link in radar signal processing and realized the suppression of false targets. In [33], the antijamming ability was improved by joint optimization of transmission polarization and transmission frequency step interval. Reference [34] adopted a method based on eigenvector to improve jamming suppression ability.

This study, according to the analysis of the principle of RGPO, takes advantage of the characteristic that the amplitude of RGPO signal is larger than the amplitude of the real target echo, a method is proposed for the FDA-MIMO radar to eliminate RGPO corresponding to the large eigenvalue, which improves the antijamming ability of the radar system and keeps the stable tracking.

The structure of this article is as follows: Section 2 introduces the signal model and the fundamentals of FDA-MIMO radar followed by the introduction of the algorithm to eliminate the jamming signal with range constraint in Section 3. Subsequently, simulation and analysis are given in Section 4. Finally, Section 5 draws a conclusion and summarizes this study.

Notation: $\otimes$ and $\odot$ denote Kronecker product and Hadamard product, respectively. The letter $j \triangleq \sqrt{-1}$ represents the imaginary unit. The transpose and conjugate transpose of a matrix or vector are denoted by $(\cdot)^T$ and $(\cdot)^H$. Boldfaced lowercase letters such as x represent a vector, boldfaced uppercase letters such as R denote a matrix, and italic letters such as a represent a scalar. For the vector x, we use $[x]_n$ to denote the nth element of vector x. For matrix R, we use $[R]_{m,n}$ to denote the element of R in the mth row and the nth column. Finally, $[a, b]$ indicates a closed interval in real number space.

2. Fundamentals of FDA-MIMO Radar

It is considered that the FDA-MMO radar system is an isometric linear array composed of M transmitting antenna elements and N receiving antenna elements [35]. Under the condition of ignoring the antenna element pattern and array error, the transmitting and receiving antenna elements are omni-directional radiation, which are identical and uniform. The transmission signal form of the mth transmitting unit can be written as [36]

$$s_m(t) = rect\left(\frac{t}{T_p}\right)\varphi_m(t)\exp\{j2\pi f_m t\}, \tag{1}$$

where t is the elapsed time of pulse propagation since the start of the pulse, $rect(t/T_p) = \begin{cases} 1, 0 \le t \le T_P \\ 0, else \end{cases}$ is the pulse modulation function, $\varphi_m(t)$ is the baseband modulation signal corresponding to the mth transmitting unit [37], and f_m is the transmitting frequency corresponding to the mth transmitting unit:

$$f_m = f_0 + (m-1)\Delta f, \quad m = 1, 2, ..., M, \tag{2}$$

where f_0 is the frequency of the reference array element (the first array element) and Δf is the frequency offset between array elements.

Assuming that there is a target at a certain position (R, θ) in space, the echo from the mth transmitting antenna unit received by the nth receiving antenna unit can be written as

$$\begin{aligned} x_{s,m,n}\left(t-\tau_{m,n}\right) = \beta_{s0} rect\left(\frac{t-\tau_{m,n}}{T_p}\right)\varphi_m\left(t-\tau_{m,n}\right) \\ \cdot \exp\left\{j2\pi f_0\left(t-\tau_{m,n}\right)\right\}, \end{aligned} \tag{3}$$

where β_{s0} represents the complex coefficient of the target echo including the full link of radar transmitting and receiving, $\tau_{m,n} = \tau_0 - d(m-1)\cos(\theta)/c - d(n-1)\cos(\theta)/c$ represents the echo delay difference corresponding to the mth transmitting unit and the nth receiving unit, and d is the interelement spacing. Because the working frequency of each transmitting element of FDA-MIMO radar is different, when equation (3) expresses the approximate model under the assumption of far-field narrowband, the phase term introduced by frequency stepping cannot be ignored. When equation (1) is brought into equation (3), we can get

$$\begin{aligned} x_{s,m,n}(t-\tau_0) \approx \beta_{s0} rect\left(\frac{t-\tau_0}{T_p}\right)\exp\{j\phi_m(t-\tau_0)\} \\ \cdot \exp\left\{j2\pi\Delta f(m-1)\left(t-\tau_{m,n}\right)\right\} \\ \cdot \exp\left\{j2\pi f_0\left(t-\tau_{m,n}\right)\right\}, \end{aligned} \tag{4}$$

where $\tau_0 = 2R/c$ is the reference delay of the target echo. The target echo received by the nth receiving antenna unit can be approximately written as

$$\begin{aligned} x_{s,n}(t-\tau_0) \approx \sum_{m=1}^{M} \beta_{s0} rect\left(\frac{t-\tau_0}{T_p}\right)\exp\{j\phi_m(t-\tau_0)\} \\ \cdot \exp\left\{j2\pi\Delta f(m-1)\left(t-\tau_{m,n}\right)\right\} \\ \cdot \exp\left\{j2\pi f_0\left(t-\tau_{m,n}\right)\right\}. \end{aligned} \tag{5}$$

The target echo is amplified and matched filtered, and the range unit where the target is located can express the signal as a concise form:

$$s = \beta_s a(R,\theta) \otimes b(\theta), \tag{6}$$

where β_s represents the complex coefficient of the target echo after pulse compression; $a(R,\theta)$ and $b(\theta)$ are the transmit and receive steering vectors of the target, respectively, and $\otimes$ is the Krnoecker product:

$$\begin{aligned} a(R,\theta) = a_r(R) \odot a_\theta(\theta) = \\ \cdot \left[1,\ \exp\left(-j4\pi\Delta f \frac{R}{c}\right), \ldots,\ \exp\left(-j4\pi\Delta f \frac{(M-1)R}{c}\right)\right]^T \odot \\ \cdot \left[1.\ \exp\left(j2\pi \frac{d\ \sin\ \theta}{\lambda}\right), \ldots,\ \exp\left(j2\pi \frac{(M-1)d\ \sin\ \theta}{\lambda}\right)\right] = \\ \cdot \left[1,\ \exp\left\{-j4\pi \frac{\Delta f R}{c} + j2\pi \frac{d}{\lambda}\cos(\theta)\right\}, \cdots,\ \exp\left\{-j4\pi \frac{\Delta f R}{c}(M-1) + j2\pi \frac{d}{\lambda}(M-1)\cos(\theta)\right\}\right]^T, \end{aligned} \tag{7}$$

$$b(\theta) = \left[1,\ \exp\left\{j2\pi \frac{d}{\lambda}\cos(\theta)\right\}, \cdots,\ \exp\left\{j2\pi \frac{d}{\lambda}(N-1)\cos(\theta)\right\}\right]^T, \tag{8}$$

where $\odot$ denotes the Hadamard product, $a_r(R)$ and $a_\theta(\theta)$ mean the launch range and launch angle steering vectors, respectively [38], and T is the transpose operator. As can be seen from equation (7), compared with the traditional radar, the range guidance vector of FDA-MIMO radar contains the range information R of the target signal, and its range guidance vector is correlated with angle and range in two dimensions. Because of the two-dimensional correlation between angle and range, FDA-MIMO radar has the ability to distinguish targets with different ranges in the transmitting space, that is, it can distinguish different targets on the close range gate with the same angle, which provides great practical value for radar to counter the jamming from mainlobe.

Assuming that airborne ESM on space far-field target intercepts radar tracking signal and releases self-defense RGPO, the intercepted radar signal is stored and transmitted with the delay to form a false target jamming signal in the fast time dimension. The jamming signal is stronger than the target echo, and the signal form corresponding to the mth transmitting unit and the nth receiving unit can be expressed as the signal form of the mth transmitting unit and the nth receiving unit:

$$x_{j,m,n}(t-\tau_j) \approx \beta_{j,p} rect\left(\frac{t-\tau_j}{T_p}\right) \exp\left\{j\phi_m(t-\tau_j)\right\} \exp\left\{j2\pi\Delta f(m-1)\left(t-\tau_{j,m,n}\right)\right\} \exp\left\{j2\pi f_0\left(t-\tau_{j,m,n}\right)\right\}, \tag{9}$$

where $\tau_j = R_i/c$ is the reference delay of the RGPO jamming signal generated by the jammer and $\tau_{j,m,n} = \tau_j - d(m-1)\cos(\theta)/c - d(n-1)\cos(\theta)/c$ represents the echo delay difference between the mth transmitting unit and the nth receiving unit.

As can be seen from equation (9), the pull-off jamming signal of the range map is completely consistent with the target echo. The time delay between the target echo and jamming is different. After the above analysis of RGPO, the jamming delay signal τ_j and the real target echo delay time τ_0 are located in the same range gate. According to the traditional radar processing method, the radar range tracking center will be greatly affected. It is necessary to combine the radar prior knowledge and jamming characteristics to design antijamming. The specific analysis is introduced in the next section. For the convenience of description, the output signal form after matched filtering is given after considering the target signal, jamming, and noise comprehensively

$$x(t) = s(t) + j(t) + n(t) = \beta_s(t) a(R,\theta) \otimes b(\theta) + \beta_j(t) a\left(R_j,\theta\right) \otimes b(\theta) + n(t). \tag{10}$$

Among them, $\beta_s(t) = \beta_s \delta(t - \tau_0)$ is the time delay corresponding to the range gate where the target located is τ_0 and $\beta_j(t) = \beta_j \delta(t - \tau_j)$ is the time delay of the jammer generating RGPO is τ_j.

3. Principle and Method of Anti-RGPO for FDA-MIMO Radar

In Section 2, the real target echo and jamming signal in FDA-MIMO radar system are studied. The echo of the target releasing self-defense jamming is completely consistent with the jamming signal in angle dimension, but its range dimension is slightly deviated. Whether the range dimension deviation can be effectively used to suppress the jamming is the key to resist this kind of mainlobe jamming. Based on the analysis of jamming mechanism and mathematical model, combined with radar signal and information processing flow, this section expounds the application of FDA-MIMIO radar against RGPO in range dimension and gives the antijamming conditions and methods.

3.1. Mechanism of RGPO. RGPO is a kind of self-defense jamming. Usually, the airborne ESM system intercepts the radar radiation signal after finding that it is tracked and locked by the tracking and guidance radar and forwards the jamming signal with a certain delay through fast storage, so that the range tracking gate center of the enemy radar deviates from the real target and locks on the released false target, thus tracking the lost technical method. In the actual radar system, after tracking the target, the angle, range, and speed of the target can be predicted with high data rate, and the target position at the next moment can be interception in a certain range, which is called wave gate. If the jamming signal deviates greatly from the real target and exceeds the wave gate range, it may be eliminated as outliers or cannot form an effective jamming track in the data processing stage, and the jamming effect would not be achieved.

RGPO can be divided into front-gate-pull-off jamming and back-gate-pull-off jamming according to different delay time functions [39]. For the jamming in front of the wavefront, the forwarding delay of the jamming signal gradually decreases for the radar tracking system, which results in an "illusion" that the false target is gradually approaching the radar system relative to the real target. For the back-gate-pull-off jamming, the delay of jamming signal forwarding increases gradually, resulting in a "phenomenon" that the range the false target is gradually apart from the real target in radar system. As for that front-gate-pull-off jamming, one or more pulse repetition stages need to be delayed. If the radar adopts frequency agility technology, the jamming effect would not be achieved. For back-gate-pull-off jamming, the time delay of the jamming signal needs to be within the same range gate as the target echo. If the radar adopts leading edge tracking technology, it can also effectively resist deceptive jamming. However, for the radar system, the time delay of the real echo received is inaccurate, and it is impossible to accurately determine the jamming style it is, so a new antijamming technology is needed to deal with the pull-off jamming with different ranges. This study focuses on countering the back-gate-pull-off jamming, and the proposed algorithm is also suitable for the front-gate-pull-off jamming.

For RGPO, it is generally divided into three stages: interception stage, pull-off stage, and stop stage:

Interception stage: after intercepting the tracking signal, the airborne ESM system stores and quickly forwards a jamming signal. Usually, the time delay of the jamming signal needs to basically coincide with the target echo in time dimension. A_s represents the amplitude of the target echo and A_j represents the amplitude of the jamming signal $A_j/A_s \approx 1.3 \sim 1.5$

Pull-off stage: in order to make the range gate center of radar deviate from the real echo of the target and avoid two echo peaks at the same time, ESM system needs to gradually increase the delay time of forwarding every time it intercepts a radar tracking signal, so that the range gate center gradually leaves the target position until the range gate deviates from the target echo by a predetermined range.

Stopping stage: when the ESM system judges that the radar has deviated from the real target by enough range from the center of the wave gate, it stops radiating jamming signals, which leads to the radar losing the target or increasing the tracking error, so it is necessary to search and find the target again.

If the above three steps are repeated, the radar can get rid of the tracking of the target or increase the tracking error of the radar.

3.2. Mathematical Model of RGPO. RGPO is mainly aimed at the radar working in tracking mode. Because the tracking filter has started to work, the radar has a priori information about the position and speed of the target, and through this priori information, the three-dimensional information of the target in the next working cycle can be predicted. In order to get rid of radar tracking, the target releases RGPO. Assuming that the pull-off range of RGPO to the center of echo is ΔR at the i pulse repetition interval (PRI) of radar, the time delay of radar receiving jamming signal is

$$\tau_j = \tau_{s,i} + \Delta\tau_{j,i}. \tag{11}$$

In the equation, τ_j is the delay time of the jamming signal [40], $\tau_{s,i}$ is the delay time of the real target echo, $\Delta\tau_{j,i} = \Delta R/c$ is the time corresponding to the pull-off jamming range of the i frame, and $\tau_{j,i} > \tau_{j,i-1}$. The pull-off range gradually increases, as shown in Figure 1.

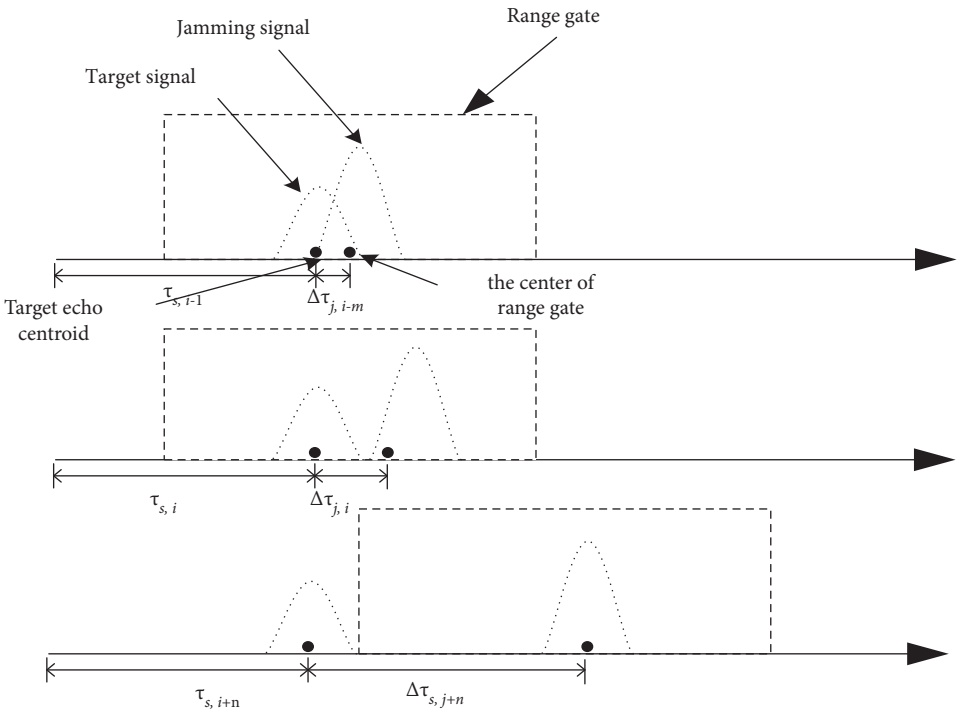

Figure 1: Schematic diagram of RGPO.

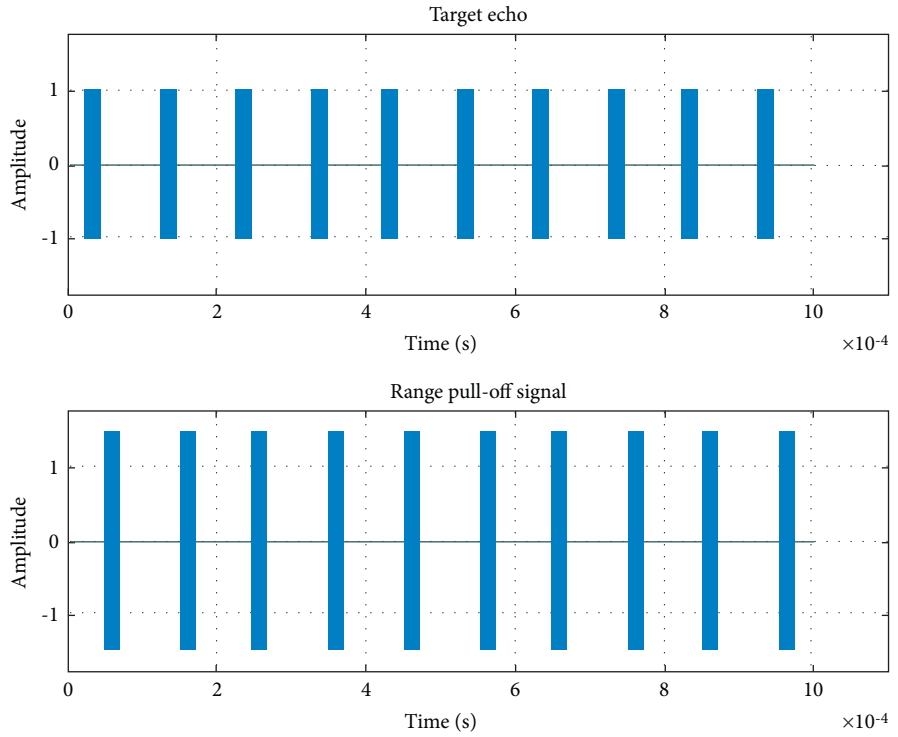

Figure 2: Schematic diagram of time domain waveform of RGPO signal.

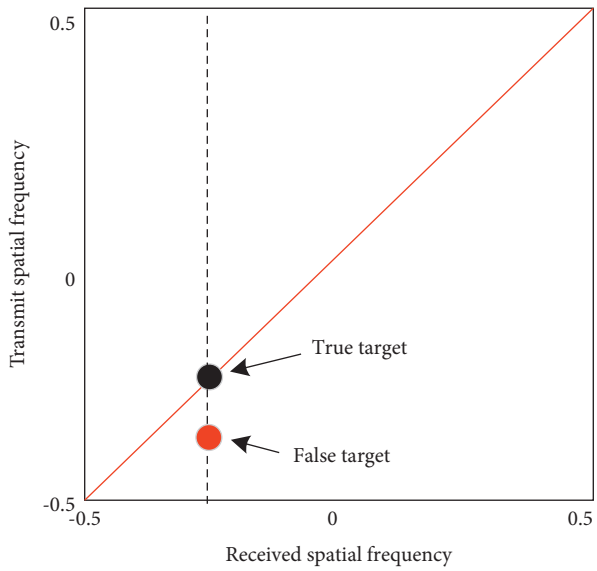

Figure 3: Distribution of real target and false target in transmitting-receiving two-dimensional spatial frequency domain after range pull-off.

The time delay information $\Delta\tau_{j,i}$ of false target caused by range gate RGPO jamming can be expressed as

$$\Delta\tau_{j,i} = \begin{cases} 0 & 0 \le i < \text{m Interception stage}, \\ \dfrac{2v(i-m)}{c} \text{ or } \dfrac{a(i-m)^2}{c} & m \le i < \text{n Pull} - \text{off stage}, \\ & n \le i < T \text{Stopping stage}. \\ \text{Pull} - \text{off stop}, & \end{cases} \tag{12}$$

Among them, a represents the pull-off acceleration in the process of uniform acceleration pull-off and v is the pull-off speed in the process of uniform acceleration pull-off. Figure 2 is a schematic diagram of time domain waveform of RGPO signal.

3.3. Jamming Suppression Method. It can be concluded that the RGPO has the following characteristics:

Feature 1: in order to deviate the center of radar gate, the amplitude of RGPO signal must be greater than the amplitude of real target echo

Feature 2: because the jamming signal and the target echo are basically consistent in time dimension during the interception stage, the jamming suppression processing cannot be carried out in time domain during the interception stage

Feature 3: during the pull-off stage, because the jamming signal gradually deviates from the target echo, the delay time of the jamming signal is different from that of the target real echo in time dimension

Assuming that the jamming parameter is (R_j, θ_j) and the transmitting space frequency and receiving space corresponding to the jamming signal are, respectively,

$$f_{Tj} = -\frac{2\Delta f R_j}{c} + \frac{d}{\lambda}\cos\left(\theta_j\right), \tag{13}$$

$$f_{Rj} = \frac{d}{\lambda}\cos\left(\theta_j\right). \tag{14}$$

Assume that the parameter of the target is (R_s, θ_s), where $\theta_s = \theta_j$, $R_s = R_j - \Delta R$, and ΔR are the pull-off range.

Then, the transmitting spatial frequency and receiving spatial frequency corresponding to the target scattering signal are

$$f_{Ts} = -\frac{2\Delta f R_s}{c} + \frac{d}{\lambda}\cos\left(\theta_s\right), \tag{15}$$

$$f_{Rs} = \frac{d}{\lambda}\cos\left(\theta_s\right). \tag{16}$$

It can be seen from the above equation that for RGPO, the receiving spatial frequency is completely consistent with the backscattered signal of the target, but the transmitting spatial frequency is different. In order to ensure the difference of transmitting spatial frequencies, the jamming suppression algorithm proposed in this study is mainly completed during the pull-off stage.

Because the release time of RGPO is that the radar has been working in the target tracking state, the relevant prior information of the target has been obtained, including the distance and angle of the target. It is assumed that the predicted position of the radar for the target is (R_y, θ_y), and the target and jamming position are extended and constrained, so that the jamming and target signals fall into the constrained range. The specific method is to set the range tracking accuracy of the radar to be σ_R. Centered on the target position predicted by the radar, and search inside $R_l = \pm 3\sigma_R$, namely:

$$\begin{cases} R_s \in \left[R_y - R_l, R_y + R_l\right] = R_h \\ R_j \in \left[R_y - R_l, R_y + R_l\right] = R_h \end{cases}, \tag{17}$$

where R_l is the range constraint value and R_h is the range in the constructed target steering vector.

According to the working principle of RGPO, assuming that the jammer releases a pull-off signal that is greater than the target echo amplitude, the covariance matrix R_X of the constrained azimuth echo can be expressed by eigenvector:

$$R_X = \sum_{k=1}^{2} \lambda_k u_k u_k^H + \sum_{k=3}^{N^2} \lambda_k u_k u_k^H. \tag{18}$$

The first term of equality coordinates u_k is the eigenvector corresponding to the signal subspace and λ_k is the eigenvalue corresponding to the signal subspace. Under the ideal condition of not considering false alarm, because the echo and jamming signal are independent,

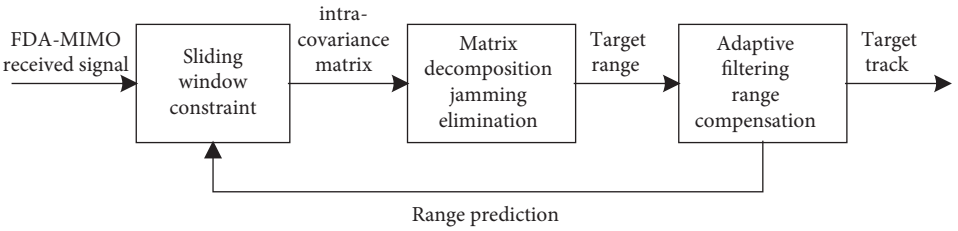

Figure 4: Flowchart of FDA-MIMO radar anti-RGPO.

Table 1: Radar simulation parameters.

Parameter	Parameter value	Parameter	Parameter value
Operating frequency	10 GHz	Pulse repetition frequency	10 kHz
Sampling frequency	5 MHz	Number of receiving array elements	10
Number of transmitting array elements	10	Receiving array element spacing	0.015 m
Launching element spacing	0.015 m	Range tracking error	40 m
Target state noise	20 m	Target motion model	Constant velocity model
SNR	10 dB	Tracking filter	Standard Kalman
Target range	10 km	Target angle	0°
RGPO JNR	15 dB	Target speed	100 m/s
Pull-off time	30 s	Range pull-off speed	10 m/s

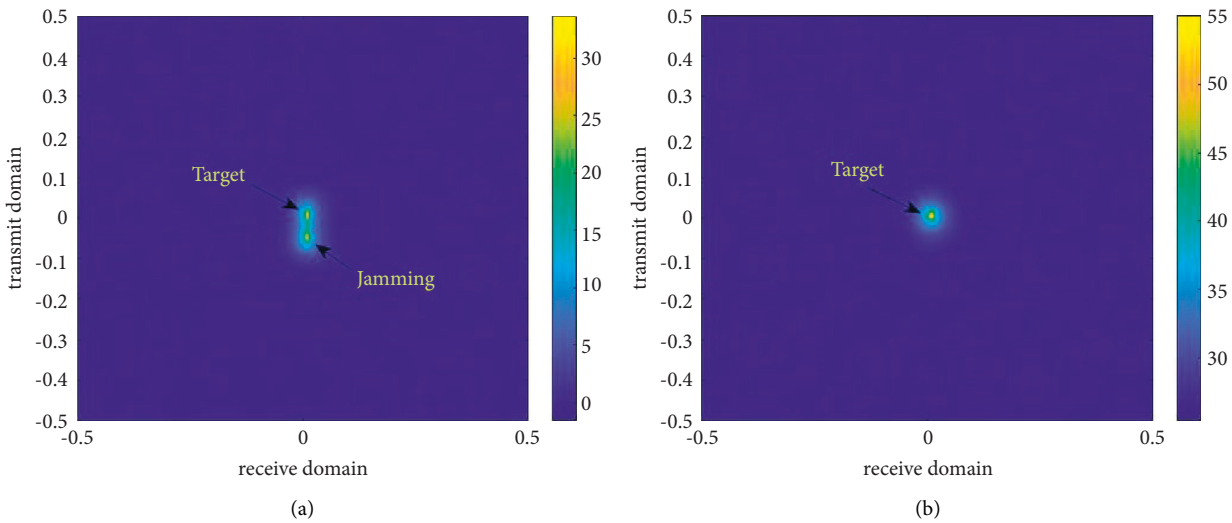

Figure 5: Power spectrum characteristics of real target and pull-off jamming. (a) Power spectrum pull-off by range. (b) Power spectrum after antijamming.

two large eigenvalues can be obtained after the eigen-decomposition of the received covariance matrix. Because the signal strength of pull-off jamming is stronger than that of target echo. The eigenvalues are arranged in sequence from large to small, the jamming signal corresponding to the largest eigenvalue is eliminated, and the rest is the range corresponding to the target signal, and then the transmission angular frequency compensation is carried out according to the range of the target signal. The transmission spatial frequencies of the compensated target signal and the pull-off jamming signal are as follows:

$$\widehat{f}_{Ts} = \frac{d}{\lambda}\cos(\theta_s), \tag{19}$$

$$\widetilde{f}_{Tj,p} = -\frac{2\Delta f \Delta R}{c} + \frac{d}{\lambda}\cos(\theta_j). \tag{20}$$

After compensation, the pull-off jamming signal can be clearly distinguished from the target signal, as shown in Figure 3.

As shown in the figure, the real target is distributed diagonally in the transmit-receive spatial frequency, and the pull-off jamming needs to deviate from the center of the gate,

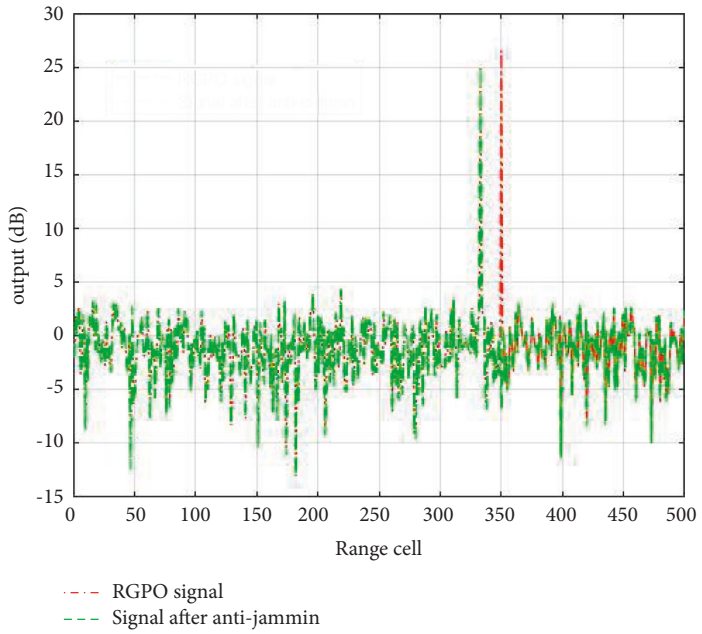

Figure 6: Output results of signal processing before and after antijamming.

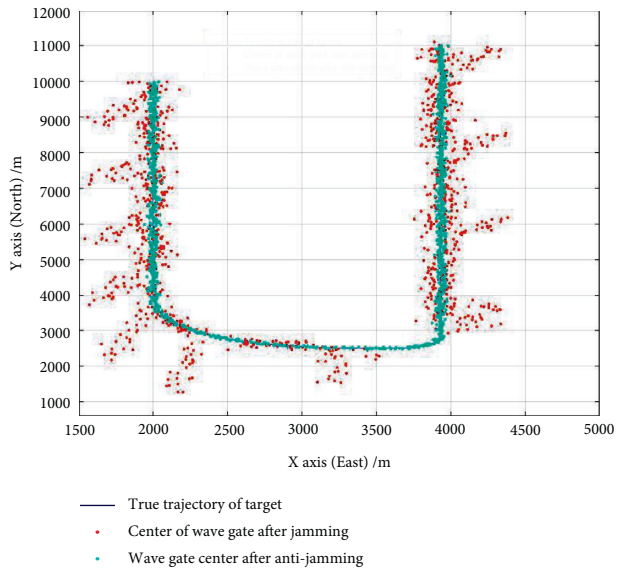

Figure 7: Change of wave gate center before and after radar jamming.

which is obviously different from the real target in the transmit spatial frequency.

Based on the analysis of real target and RGPO signal characteristics, combined with the characteristics of FDA-MIMO radar, two-dimensional beamforming technology is used to suppress pull-off jamming signal. Its beamformer weights can be expressed as

$$w_{MF} = a\left(\widehat{f}_T\right) \otimes b\left(\widehat{f}_R\right). \tag{21}$$

After the target range compensation, the weights of the two-dimensional filter are independent of the range parameters, but only related to the angle parameters of radar detection. However, the weights of two-dimensional filters are affected by the following two factors:

(1) The accuracy of radar prediction of target range, which would cause the loss of matching output

(2) The accuracy of radar angle estimation, which directly affects the accuracy of weights

The adaptive beamformer based on the minimum lossless response criterion can overcome the above influence factors, which can be expressed as

$$\begin{aligned} &\min_{w_{AMF}} E\left\{\left|w_{AMF}^H \tilde{x}\right|^2\right\} \\ &s.t. w_{AMF}^H \left[a\left(\widehat{f}_T\right) \otimes b\left(\widehat{f}_R\right)\right] = 1. \end{aligned} \tag{22}$$

where $\tilde{x}$ is the compensated data. After adaptive beamforming, the influence of range gate pull-off jamming can be effectively suppressed.

In this study, the flow of the specific method proposed is shown in Figure 4:

Step 1: use the radar's predicted value of the target range dimension to constrain the target steering vector according to equation (16), and set the constraint range to within $\pm 3\sigma_R$ the radar tracking accuracy, so that the real target and the jamming signal are both within the constrained steering vector range;

Step 2: perform eigendecomposition on the covariance matrix R_X, including the target echo and the jamming signal, and use the characteristic that the jamming signal is stronger than the target echo to eliminate the jamming signal range corresponding to the large eigenvalue to obtain the true range of the target;

Step 3: after obtaining the true range of the real target, compensate the launch angle frequency, distinguish the jamming signal and the target echo in the launch-receive spatial frequency, use the MVDR criterion to form an adaptive filter, complete the range

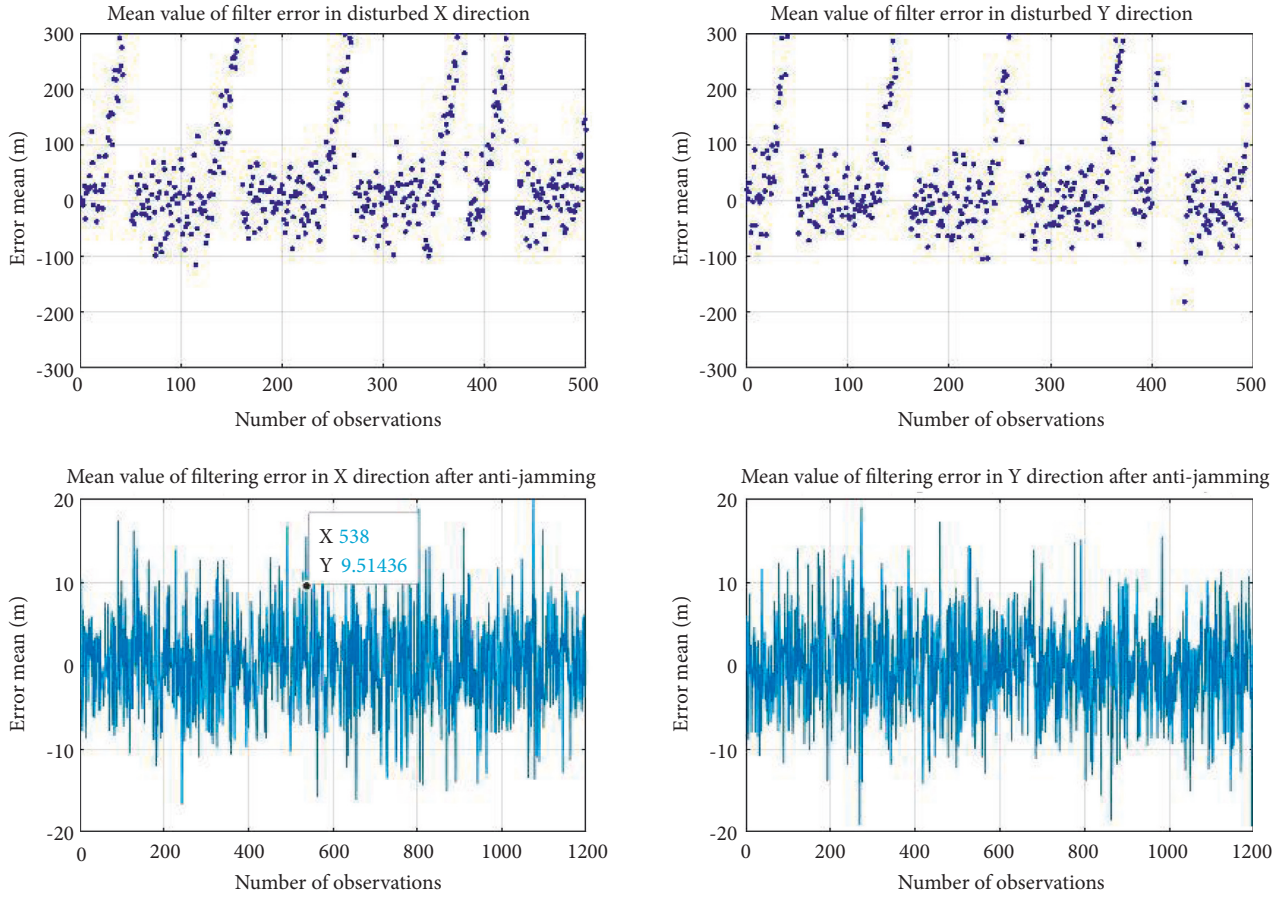

Figure 8: The average change of tracking error before and after radar antijamming.

compensation in the launch dimension, and complete the target track.

4. Simulation Verification

In this section, the effectiveness of the proposed approach is verified by simulation examples. Without losing generality, assume that the radar receives the jamming signal radiated by the enemy when it has stably tracked the target, and the jammer intercepts the radar tracking signal and tows it to release the RGPO. The relevant parameters of simulation are given in Table 1.

4.1. Power Spectrum Analysis before and after Antijamming. Figure 5 shows the simulation comparison results of echo before and after processing the antijamming approach proposed in the transmission-reception frequency domain. It can be seen from the simulation results that because the echo in FDA-MIMO system contains the range dimension information of the echo in the transmitting frequency domain, the radar cannot accurately distinguish the real target echo because the amplitude of the jamming signal is greater than that of the echo after receiving the RGPO signal, and the range between the jamming signal and the target echo is close during the pull-off stage. After constrained and large signal is proposed, the transmission frequency domain can be compensated, and the true echo of the target can be accurately detected. It should be noted that due to the target motion and radar detection error, the position of the compensated target may change slightly. Figure 6 shows the signal strength distribution after pulse compression in range dimension before and after antijamming. In this simulation, with receiving the jamming signal, the maximum amplitude of the output is about 28 dB and the range cell is 350 where the jamming is, after processing antijamming, the maximum amplitude of the output is about 25 dB and the range cell is 333 where the real target is.

4.2. Tracking Performance Analysis. The tracking performance before and after antijamming is analyzed. In order to accurately show the experimental results, it is assumed that the flying height of the target remains unchanged in the northeast coordinate system, and the tracking performance is mainly analyzed on X axis and Y axis. Figure 7 shows the change of the whole range segment of the range-dimensional tracking gate center before and after the radar is jammed by range pull-off. It can be seen from the example that after receiving the RGPO, the range tracking gate center of the radar would gradually deviate from the real target position, resulting in increased tracking error or even out of tolerance, and the target would be lost after the jamming signal disappears. Figure 8 shows the average tracking error of X axis

and Y axis in the radar tracking process. It can be seen that the tracking error increases dramatically after receiving the RGPO. After filtering, the two-dimensional range error is about ±300 m, which is far greater than the radar tracking accuracy. After antijamming, the two-dimensional range error changes ±40 m, and the radar can keep stable tracking of the target.

5. Conclusion

Tracking and guidance radar is usually affected by the mainlobe jamming. In this study, focused on the principle and application of FDA-MIMO radar against range gate pull-off jamming, an effective way to solve the problem that the center of range gate deviates from the real target greatly due to pull-off jamming is provided on the basis of analyzing the principle and working process of RGPO. Based on two-dimensional transceiver beamforming and range eliminating, the jamming signal can be suppressed. The experimental results verify the effectiveness and feasibility of the proposed method from two important links of detection and tracking radar.

Data Availability

The data used to support the findings of this study are available from the corresponding author upon request.

Conflicts of Interest

The authors declare that there are no conflicts of interest.

Acknowledgments

This work was supported by the Nature Science Foundation of China (NSFC) (61931016).

References

[1] G. Li, Y. Zhou, W. Xia, and J. Cao, "A Simulation Technique Service Training Method of Guidance Radar Equipment Based on Visual Simulation," in *Proceedings of the 2016 2nd IEEE International Conference on Computer and Communications (ICCC)*, pp. 2864–2868, Chengdu, October 2016.

[2] D. Tarchi, F. Oliveri, and P. F. Sammartino, "MIMO radar and ground-based SAR imaging systems: equivalent approaches for remote sensing," *IEEE Transactions on Geoscience and Remote Sensing*, vol. 51, no. 1, pp. 425–435, January. 2013.

[3] A. Basit, S. Y. Nusenu, S. Wali, and S. Wali, "FDA based QSM for mmWave wireless communications: frequency diverse transmitter and reduced complexity receiver," *IEEE Transactions on Wireless Communications*, vol. 20, no. 7, pp. 4571–4584, 2021.

[4] X. Li, D. Wang, X. Ma, and W. Q. Wang, "FDS-MIMO radar low-altitude beam coverage performance analysis and optimization," *IEEE Transactions on Signal Processing*, vol. 66, no. 9, pp. 2494–2506, 2018.

[5] A. Basit, S. Y. Nusenu, S. Wali, and S. Yaw Nusenu, "Transmit beamspace design for FDA–MIMO radar with alternating direction method of multipliers," *Signal Processing*, vol. 180107832 pages, 2021.

[6] M. Soumekh, "SAR-ECCM using phase-perturbed LFM chirp signals and DRFM repeat jammer penalization," *IEEE Transactions on Aerospace and Electronic Systems*, vol. 42, no. 1, pp. 191–205, January. 2006.

[7] L. Lan, M. Rosamilia, A. Aubry, A. D. Maio, and G. Liao, "Single-snapshot angle and incremental range estimation for FDA-MIMO radar," *IEEE Transactions on Aerospace and Electronic Systems*, vol. 57, no. 6, pp. 3705–3718, 2021.

[8] L. Lan, G. Liao, J. Xu, Y. Zhang, and B. Liao, "Transceive beamforming with accurate nulling in FDA-MIMO radar for imaging," *IEEE Transactions on Geoscience and Remote Sensing*, vol. 58, no. 6, pp. 4145–4159, 2020.

[9] S. Zhao and Z. Liu, "Main-Lobe jamming suppression method in multiple-radar system," in *Proceedings of the IGARSS 2019 IEEE International Geoscience and Remote Sensing Symposium*, pp. 2276–2279, Yokohama, Japan, August 2019.

[10] Z. Xiang, B. Chen, and M. Yang, "Polarization optimization for mainlobe interference suppression," *International Conference on Radar Systems (Radar)*, vol. 12, pp. 1–5, 2017.

[11] Y. Yuan, G. Cui, M. Ge, X. Yu, and L. Kong, "Active repeater jamming suppression via multistatic radar elliptic-hyperbolic location," *Proc. IEEE Radar Conference*, vol. 45, pp. 692–697, May 2017.

[12] F. Bandiera, A. Farina, D. Orlando, and G. Ricci, "Detection algorithms to discriminate between radar targets and ECM signals," *IEEE Transactions on Signal Processing*, vol. 58, no. 12, pp. 5984–5993, December, 2010.

[13] G. Zheng, Y. Song, and C. Chen, "Height Measurement for with wave polarimetric MIMO radar: signal model and MUSIC algorithm," *Signal Processing*, vol. 190, 2022.

[14] P. Wan, Y. Weng, J. Xu, and G. Liao, "Range gate pull-off mainlobe jamming suppression approach with FDA-MIMO radar theoretical formalism and numerical study," *Remote Sensing*, vol. 14, no. 6, p. 1499, 2022.

[15] J. Shi, Z. Yang, and Y. Liu, "On parameter identifiability of diversity-smoothing-based MIMO radar," in *IEEE Transactions on Aerospace and Electronic Systems*, November 2021.

[16] J. Zhang, X. Zhu, and K. E. Wang, "A waveform diversity technique for countering RGPO," *2009 IET International Radar Conference*, vol. 58, pp. 1–4, 2009.

[17] T. Cheng, Z. He, and Y. Li, "An Effective Target Tracking Algorithm with Anti-RGPO Ability," in *Proceedings of the 10th IEEE International NEWCAS Conference*, pp. 117–120, Montreal, QC, Canada, June 2012.

[18] X. Yong, Y. Fang, S. Chen, and Y. Wu, "Sensor registration algorithm considering RGPO deception," *2015 Chinese Automation Congress (CAC)*, vol. 6, pp. 1874–1878, 2015.

[19] R. Jia, T. Zhang, Y. Wang, and Y. Deng, "An Intelligent Range Gate Pull-Off (RGPO) Jamming Method," in *Proceedings of the 2020 International Conference on UK-China Emerging Technologies*, pp. 1–4, UCET), Glasgow, UK, August 2020.

[20] M. Greco, F. Gini, and A. Farina, "Combined effect of phase and RGPO delay quantization on jamming signal spectrum," *IEEE International Radar Conference*, vol. 77, pp. 37–42, 2005.

[21] M. T. Öztürk, Y. Dalveren, and A. Kara, "Spectrum analysis of parabolic range gate pull-off (RGPO) signals," in *Proceedings of the 2015 23nd Signal Processing and Communications Applications Conference (SIU)*, pp. 1026–1029, Malatya, Turkey, May 2015.

[22] M. Xie, L. Liu, C. Zhang, and X. Fu, "Bidirectional false targets RGPO jamming," in *Proceedings of the 2018 13th IEEE Conference on Industrial Electronics and Applications (ICIEA)*, pp. 2345–2348, Wuhan, China, May 2018.

[23] G. Rui-xing and Z. Jian-yun, "Jamming power compensate method related to RGPO retransmission time delay," *Fire Control and Command Control*, vol. 43, no. 06, pp. 107–110+117, 2018.

[24] y. Xue and Ai ping Yang, "Analysis and simulation of range gate pull jamming method based on frequency," *ShiftShipboard Electronic Countermeasure*, vol. 41, no. 03, pp. 42–44+95, 2018.

[25] J. Xiong, W. Q. Wang, and K. Gao, "FDA-MIMO radar range-angle estimation: CRLB, MSE, and resolution analysis," *IEEE Transactions on Aerospace and Electronic Systems*, vol. 54, no. 1, pp. 284–294, February. 2018.

[26] L. Lan, J. Xu, G. Liao, Y. Zhang, F. Fioranelli, and H. C. So, "Suppression of mainbeam deceptive jammer with FDA-MIMO radar," *IEEE Transactions on Vehicular Technology*, vol. 69, no. 10, pp. 11584–11598, 2020.

[27] J. Xu, S. Zhu, and G. Liao, "Range ambiguous clutter suppression for airborne FDA-STAP radar," *IEEE Journal of Selected Topics in Signal Processing*, vol. 9, no. 8, pp. 1620–1631, December, 2015.

[28] J. Xu, G. Liao, Y. Zhang, H. Ji, and L. Huang, "An adaptive range-angle-Doppler processing approach for FDA-MIMO radar using three-dimensional localization," *IEEE Journal of Selected Topics in Signal Processing*, vol. 11, no. 2, pp. 309–320, March 2017.

[29] G. Zheng and Y. Song, "Signal model and method for joint angle and range estimation of low-elevation target in meter-wave FDA-MIMO radar," *IEEE Communications Letters*, vol. 26, no. 2, pp. 449–453, February. 2022.

[30] L. Lan, J. Xu, S. Zhu, and G. Liao, "Advances in anti-jamming using waveform diverse array radar," *Systems Engineering and Electronics*, vol. 43, no. 6, pp. 1437–1451, 2021.

[31] J. Xu, J. Kang, G. Liao, and H. C. So, "Mainlobe Deceptive Jammer Suppression with FDA-MIMO Radar," in *Proceedings of the 2018 IEEE 10th Sensor Array and Multichannel Signal Processing Workshop (SAM)*, pp. 504–508, Sheffield, UK, July 2018.

[32] Z. Zhang and J. Xie, "Discrimination method of range deception jamming based on FDA-MIMO," *Journal of Beijing University of Aeronautics and Astronautics*, vol. 43, no. 4, pp. 738–746, 2016.

[33] R. Gao and Y. Quan, "Main-lobe decetive Jamming suppression with FDA-MIMO radar based on BSS," *Systems Engineering and Electronics*, vol. 42, no. 9, pp. 1927–1934, 2020.

[34] H. Chen and R. Li, "FDA-MIMO radar main-lobe dense false target jamming suppression based on feature vector eliminating," *Journal of Air Force Early Warning Academy*, vol. 32, no. 6, pp. 397–401, 2018.

[35] Q. Liu, J. Xu, Z. Ding, and H. C. So, "Target localization with jammer removal using frequency diverse array," *IEEE Transactions on Vehicular Technology*, vol. 69, no. 10, pp. 11685–11696, 2020.

[36] L. Lan, G. Liao, J. Xu, Y. Zhang, and F. Fioranelli, "Suppression approach to main-beam deceptive jamming in FDA-MIMO radar using nonhomogeneous sample detection," *IEEE Access*, vol. 6, pp. 34582–34597, 2018.

[37] Z. Ding and J. Xie, "Joint transmit and receive beamforming for cognitive FDA-MIMO radar with moving target," *IEEE Sensors Journal*, vol. 21, no. 18, pp. 20878–20885, 2021.

[38] J. Xu, G. Liao, S. Zhu, L. Huang, and H. C. So, "Joint range and angle estimation using MIMO radar with frequency diverse array," *IEEE Transactions on Signal Processing*, vol. 63, no. 13, pp. 3396–3410, July, 2015.

[39] H. Zhou, C. Dong, R. Wu, X. Xu, and Z. Guo, "Feature fusion based on bayesian decision theory for radar deception jamming recognition," *IEEE Access*, vol. 9, pp. 16296–16304, 2021.

[40] J. Yang, X. Fu, C. Zhang, X. Yin, P. Cong, and S. Su, "Anti-Time-Delay Repeater Jamming under Sea Surface Target Spatial Position Constraint," in *Proceedings of the 2019 IEEE 4th International Conference on Signal and Image Processing (ICSIP)*, pp. 425–429, Wuxi, China, July 2019.